JOURNAL OF APPLIED POLYMER SCIENCE VOL. 17, PP. 1203–1225 (1973)

Stratified Two-Phase Flow of Molten Polymers

THOMAS C. YU and CHANG DAE HAN, *Department of Chemical Engineering, Polytechnic Institute of Brooklyn, Brooklyn, New York 11201*

Synopsis

A study has been made of stratified two-phase flow of molten polymers in a slit die. For the experimental study, measurements were taken of wall normal stresses along the longitudinal axis of a rectangular duct which had an aspect ratio of 10. Three pressure transducers were flush-mounted on each of the rectangle's long sides, directly opposite from each other. The measurements permitted one to determine the pressure gradients of each component (their viscous properties) and the exit pressures of each component (their elastic properties). For the theoretical study, the fully developed velocity distributions of two-phase flow were determined by solving the equations of motion by use of a power law model. The volumetric flow rates, calculated theoretically by use of a power law model, are compared with experimentally observed ones. Experimental evidence is presented which clearly shows that polystyrene and polypropylene form two incompatible phases in the molten state.

INTRODUCTION

Two-phase flow has been a subject of considerable interest to many researchers during the past few decades. However, most studies were concerned with gas–liquid systems, and only a small fraction of them dealt with liquid–liquid systems. Among the studies made of liquid–liquid systems, many have dealt with Newtonian fluids, but very few with non-Newtonian viscoelastic fluids.

Two types of two-phase flow may be considered from the point of view of the manner in which phase separation occurs. One type is the dispersed two-phase system in which one component exists as a discrete phase (droplets) dispersed in the other which forms a continuous phase. The other is the stratified two-phase system in which both components form continuous phases separated from each other by a continuous boundary.

Mixtures of heavy crude oil and water flowing through long horizontal pipelines have been reported to form stratified two-phase system. In that instance, stratification occurs owing to the large differences in densities and viscosities between the heavy crude oil and water. It was reported that an addition of a small amount of water to crude oil flowing through the pipeline has considerably reduced the pressure gradient of the crude oil–water mixture, resulting in a reduction of pumping cost. This fact has apparently stimulated many theoretical and experimental studies by several investigators[1–4] who investigated stratified laminar flow of oil–water mixtures in long, horizontal tubes or rectangular ducts.

The recent development in formulating various polymer blends and composite polymeric materials has prompted many researchers to investigate the various flow problems involved with incompatible polymer systems in the molten state. It is a fact well known to the polymer processing industry that both dispersed and stratified two-phase flow occur in several important polymer processings. Two industrially important polymer systems which form dispersed two-phase flow in the molten state are rubber-reinforced polystyrene and acrylonitrile–butadiene–styrene (ABS) plastics. In both, a rubbery component is dispersed in a glassy matrix of the resin phase. Very recently, Han and Yu[5,6] demonstrated that blends of polystyrene with polypropylene and blends of polystyrene with polyethylene form two phases in the molten state when melted and extruded through capillary dies.

Typical industrial processes which make use of stratified flow of molten polymers are the production of composite materials such as conjugate (bicomponent) fibers and multilayered films. In making composite materials, separate feed streams of molten polymers meet each other at the die inlet and then flow through circular or rectangular ducts. As molten polymers possess both viscous and elastic properties, an analysis of the stratified flow of molten polymers is much more complex than that of Newtonian fluids. It is also to be noted that in general two chemically dissimilar polymers are incompatible in the molten state.

At this point it is worth mentioning that earlier there has been some important development reported on the production of conjugate fibers, which met some commercial success due to several industrial research groups, namely, Sisson and Morehead[7] and Hicks et al.[8–10] The motivation of their study was to produce crimped fibers very similar to natural wool fibers. For this purpose, Sisson and Morehead[7] spun two viscose solutions side by side through circular spinnerette holes and successfully produced crimped fibers which possess a certain degree of bilateral structure in a rayon. Similarly, Hicks et al.[8] developed the bicomponent acrylic fiber (Orlon 21) which also produced crimps due to bilateral structure in an acrylic fiber.

More recently, a few studies have been reported[11–13] which were concerned with the somewhat fundamental nature of the bicomponent stratified flow of viscoelastic fluids. Southern and Ballman[11] investigated the interfacial shape when two commercial polystyrenes were extruded side by side, whereas White et al.[12] investigated the flow patterns when two incompatible molten polymers (low-density polyethylene and polystyrene) flow side by side. Slattery[13] pressented an analysis on laminar two-phase concentric flow of the simple fluid advanced by Noll[14] and Coleman and Noll[15] in a circular tube. Slattery's analysis gives an analytical expression for relating the total volumetric flow rate to two material functions, one for each phase, which are unknown functions of the shear rate.

Unfortunately, there is scarcely any fundamental work published dealing with the stratified two-phase flow of polymer melts as applied to industrially

important polymer processing methods. It is the purpose of this paper to present the authors' recent work on this topic. The paper discusses both a theoretical and an experimental investigation made on the stratified flow of polystyrene and polypropylene melts in a slit die.

ANALYSIS

One can conceive of a variety of different types of stratified flow. For instance, such geometries as sketched in Figures 1a and 1b have been widely used in bilayered and multilayered film extrusions. Similarly, geometries such as sketched in Figure 1c and 1d have been used in manufacturing bicomponent fibers. In the following analysis, we shall consider only the geometry of Figure 1a, in order to simulate the actual experimental system chosen for study.

Figure 2 depicts the flow geometry and the coordinate system of stratified two-phase flow through a thin slit die (i.e., two parallel plates with infinite

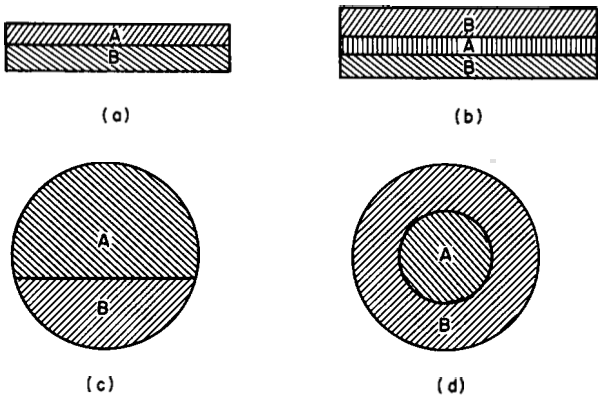

Fig. 1. Different geometries of stratified flow, which are of interest to polymer processing.

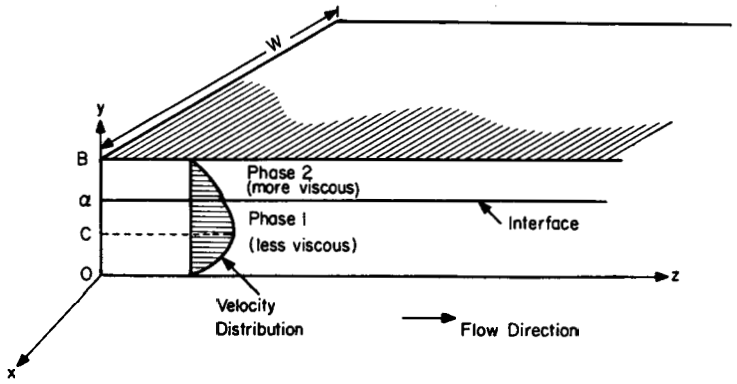

Fig. 2. Plane slit geometry.

width). For fully developed flow, the z-component of the equation of motion is given by

$$-\frac{\partial p}{\partial z}+\frac{\partial \tau_{yz}}{\partial y}=0. \tag{1}$$

Integrating eq. (1) gives
For phase 1,

$$\tau_{yz}=-P'(y-C_1) \qquad \text{for } 0\leq y<\alpha \tag{2}$$

For phase 2,

$$\bar{\tau}_{yz}=-P'(y-C_2) \qquad \text{for } \alpha<y\leq B \tag{3}$$

where C_1 and C_2 are integration constants and P' is the pressure gradient defined by $P'=-\partial p/\partial z$. Note that throughout this paper, variables *without* the overbar denote phase 1, and variables *with* the overbar denote phase 2. Note further in eqs. 2 and 3 that the pressure gradients in both phases are assumed to be the same. This assumption will be shown to be correct, both theoretically and experimentally, in a later section.

For the flow geometry under consideration (see Fig. 2), the steady-state velocity field is given by

$$\left.\begin{aligned} V_z &= V(y)=f(y) \\ V_x &= V_y=0 \end{aligned}\right\} \tag{4}$$

Now, boundary conditions may be written as follows:

(i) At $y=0$,

$$V=0 \tag{5}$$

(ii) At $y=$ B,

$$\bar{V}=0 \tag{6}$$

(iii) At $y=\alpha$,

$$V=\bar{V} \tag{7}$$

(iv) At $y=\alpha$,

$$\tau_{yz}=\bar{\tau}_{yz}. \tag{8}$$

Use of boundary condition 8 in eqs. (2) and (3) yields

$$\tau_{yz}=-P'(y-C) \text{ for } 0\leq y<\alpha \tag{9}$$

$$\bar{\tau}_{yz}=-P'(y-C) \text{ for } \alpha<y\leq B \tag{10}$$

where $C=C_1=C_2$.

In order to obtain the velocity profile and then to calculate the volumetric flow rate, one needs to choose a constitutive equation to solve eqs. (9) and (10). In the past, a number of constitutive equations have been suggested in the literature. In fact, choice of a constitutive equation is

somewhat arbitrary. For our purpose here, we choose a power law fluid because of its simplicity in subsequent mathematical manipulations.

For the velocity field given by eq. (4), a power law fluid may be written as For phase 1,

$$\tau_{yz} = K\gamma^n \tag{11}$$

where

$$\gamma = \frac{dV}{dy} \qquad \text{for } 0 \leq y \leq C \tag{12}$$

$$\gamma = -\frac{dV}{dy} \qquad \text{for } C \leq y \leq \alpha. \tag{13}$$

For phase 2,

$$\bar{\tau}_{yz} = \bar{K}\bar{\gamma}^{\bar{n}} \tag{14}$$

where

$$\bar{\gamma} = -\frac{d\bar{V}}{dy} \qquad \text{for } \alpha \leq y \leq B. \tag{15}$$

Note in eq. (11) that the shear rate γ changes its sign at the position of $y = C$, where a maximum velocity (hence zero velocity gradient, $dV/dy = 0$) occurs, as shown schematically in Figure 2.

Now, equating the right-hand sides of eqs. (9) and (11) gives

$$\gamma = [P'(C - y)/K]^{1/n} \tag{16}$$

or

$$y = C - (K/P')\gamma^n. \tag{17}$$

Differentiating eq. (17) with respect to y yields

$$dy = -(K/P')n\gamma^{n-1}d\gamma. \tag{18}$$

Integrating eq. (12) with the aid of eq. (18), one obtains

$$V(y) = \int_0^y \gamma dy = \frac{K}{P'}\frac{n}{n+1}(\gamma_0{}^{n+1} - \gamma^{n+1}) \tag{19}$$

where

$$\gamma_0 = (\gamma)_{y=0} = (P'C/K)^{1/n}. \tag{20}$$

It can be easily shown that eq. (19) is valid for the entire distance in phase 1 if γ is defined as

$$\gamma = (P'|C - y|/K)^{1/n} \qquad \text{for } 0 \leq y \leq \alpha. \tag{21}$$

In a similar manner, one can derive the velocity profile in phase 2 as follows:

$$\bar{V}(y) = \frac{\bar{K}}{P'}\frac{\bar{n}}{\bar{n}+1}(\bar{\gamma}_B{}^{\bar{n}+1} - \gamma^{\bar{n}+1}) \tag{22}$$

where

$$\bar{\gamma} = [P'(y - C)/K]^{1/\bar{n}} \quad \text{for } \alpha \leq y \leq B \tag{23}$$

$$\bar{\gamma}_B = (\bar{\gamma})_{y=B} = [P'(B - C)/\bar{K}]^{1/\bar{n}}. \tag{24}$$

It should be noted that eqs. (19) and (22) contain a constant C, yet are to be determined with the aid of boundary condition 7. That is, the equation

$$\frac{K}{P'} \frac{n}{n+1} (\gamma_0{}^{n+1} - \gamma_\alpha{}^{n+1}) = \frac{\bar{K}}{P'} \frac{\bar{n}}{\bar{n}+1} (\bar{\gamma}_B{}^{\bar{n}+1} - \bar{\gamma}_\alpha{}^{\bar{n}+1}) \tag{25}$$

should be solved for C, in which γ_α and $\bar{\gamma}_\alpha$ are to be evaluated from eqs. (21) and (23), respectively, by setting $y = \alpha$. As may be supposed, solution of eq. (25) for C requires a trial-and-error procedure using some kind of successive iteration scheme.

Once a correct value of C is found which satisfies eq. (25), one can calculate the volumetric flow rate from
For phase 1,

$$Q = W\left(\frac{K}{P'}\right)^2 \frac{n}{n+1} \left(\frac{n+1}{2n+1} \gamma_0{}^{2n+1} + \gamma_0{}^{n+1} \gamma_\alpha{}^n - \frac{n}{2n+1} \gamma_\alpha{}^{2n+1}\right) \tag{26}$$

For phase 2,

$$\bar{Q} = W\left(\frac{\bar{K}}{P'}\right)^2 \frac{\bar{n}}{\bar{n}+1} \left(\frac{\bar{n}+1}{2\bar{n}+1} \bar{\gamma}_B{}^{2\bar{n}+1} - \bar{\gamma}_B{}^{\bar{n}+1} \bar{\gamma}_\alpha{}^{\bar{n}} + \frac{\bar{n}}{2\bar{n}+1} \bar{\gamma}_\alpha{}^{2\bar{n}+1}\right). \tag{27}$$

EXPERIMENTAL

Materials

Materials chosen for the experimental study were: general-purpose polystyrene (Dow Styron 686) and polypropylene (Enjay Chemical Resin E115). The main reason for choosing these materials is that previous studies by the authors[5,6] have demonstrated that blends of these two polymers form two phases when melted and extruded through a capillary.

Apparatus and Experimental Procedure

The apparatus consists of a 1-in. Killion extruder, a Zenith gear pump driven by a variable-speed motor, a reservoir section which includes a sharp-edged flow divider, and a slit die section. Figure 3 is a photograph of the apparatus.

Two molten polymers were separately fed to the reservoir section: polypropylene from the extruder, and polystyrene from the hydraulic holding-tank (by means of a gear pump). Figure 4 shows detailed sketches of both the feed and die sections, and Figure 5 is a detailed sketch of the die, showing how the pressure transducers were mounted on the die. The

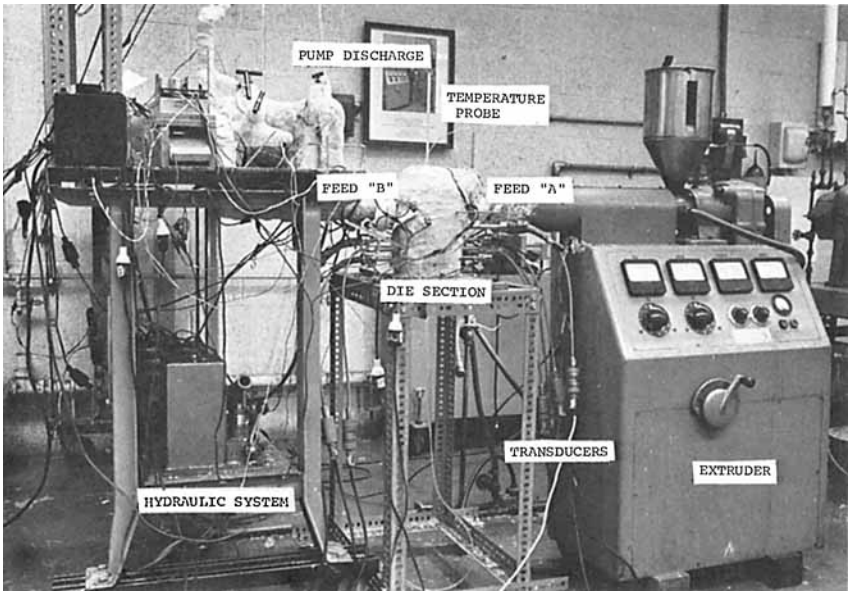

Fig. 3. Photograph of the apparatus.

hydraulic holding-tank was used to supply one of the polymers because there was only extruder available to us. This holding-tank was constructed earlier for a melt-spinning experiment, and the details of the operating procedures of the hydraulic system are given in a recent paper by Han and Lamonte.[16]

The experimental procedure was straightforward. Two polymers were fed separately to the slit die, and measurements of wall normal stress were made by means of melt pressure transducers (Dynisco Model PT 422), which were flush-mounted on each of the rectangle's long sides, directly opposite each other. When the flow was equilibrated after a new setting of flow rate, measurements were taken of wall pressures and flow rates of each polymer. The outputs of the transducers were read in millivolts by a potentiometer and null detector. The pressure transducers were calibrated against a dead weight tester. Measurements were repeatable within 1% at pressures of 25 psig and above.

In this experiment, good temperature control was crucial. The whole system was heated by Calrod tubular heaters and was heavily insulated with asbestos. Temperature was controlled within $\pm 1°F$ by Thermistor-operated thermal regulators.

RESULTS AND DISCUSSION

Wall Pressure Measurements

Table I shows measurements of wall normal stresses along the longitudinal axis of a thin slit die, through which polystyrene and polypropylene

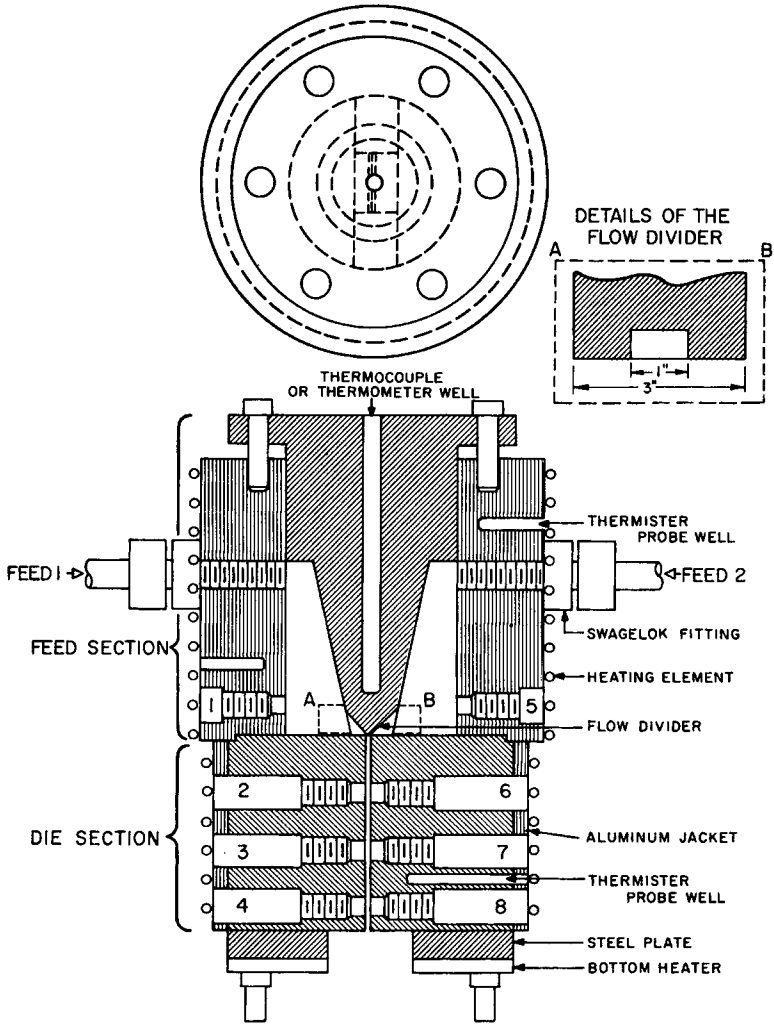

Fig. 4. Detailed layout of the die assembly.

melts flow parallel to each other. It may be seen from Table I that, within measurement error, the two pressure readings opposite each other are essentially the same over the range of the variables investigated.

In fact, one can show from the y-component of the equation of motion,

$$-\frac{\partial p}{\partial y}+\frac{\partial \tau_{yy}}{\partial y}=0, \tag{28}$$

that the wall normal stresses must be the same for both phases. Using the definition

$$S_{yy}(y,z)=-p(y,z)+\tau_{yy}(y) \tag{29}$$

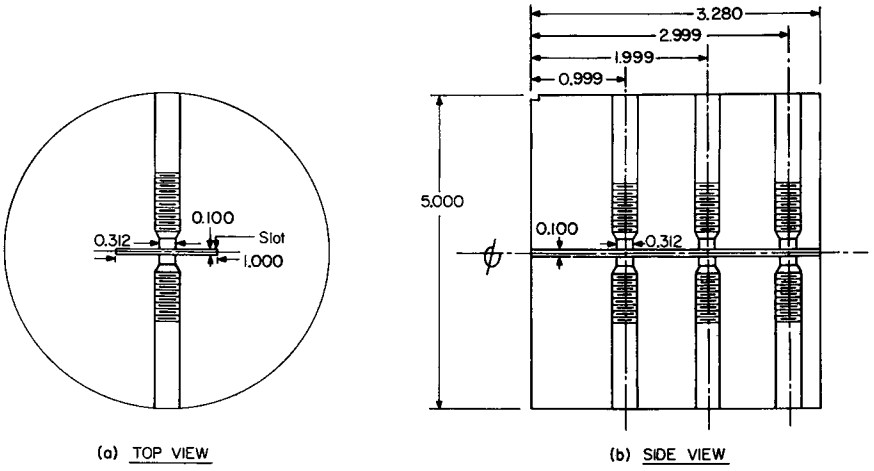

Fig. 5. Details of the slit die design.

one can rewrite eq. (28) as
For phase 1,

$$\frac{\partial S_{yy}}{\partial y} = 0 \tag{30}$$

For phase 2,

$$\frac{\partial \bar{S}_{yy}}{\partial y} = 0. \tag{31}$$

Therefore we have from eqs. (30) and (31),

$$S_{yy} = \bar{S}_{yy} = \text{constant}. \tag{32}$$

This implies that, at a fixed axial position z, the normal stresses, S_{yy} in phase 1 and $\bar{S}_{yy}$ in phase 2, are constant throughout their respective phases.

It is clear from eq. (32) that the pressures measured at the walls of the long side of the rectangle can be expected to be the same for the two phases (see Table I) because the wall pressures measured by means of transducers are nothing but the negative wall normal stresses. Since for fully developed flow the deviatoric component of normal stresses, $\tau_{yy}(y)$, is independent of z, as may be seen from eq. (29), eq. (32) suggests further that

$$\frac{\partial S_{yy}}{\partial z} = \frac{\partial \bar{S}_{yy}}{\partial z} \tag{33}$$

or

$$-\frac{\partial p}{\partial z} = -\frac{\partial \bar{p}}{\partial z} = P'. \tag{34}$$

TABLE I
Wall Pressure Measurements in the Stratified Two-Phase Flow of Polymer Melts

Run no.	Material[a]	Flow rate, cc/min	Wall pressure,[b] psig			Pressure gradient $-\partial p/\partial z$, psi/in.
			P_1	P_2	P_3	
1	PS	6.80	210.0	118.4	28.6	90.80
	PP	13.00	209.2	124.6	27.4	
2	PS	9.20	217.6	123.4	29.9	94.07
	PP	12.75	218.0	126.5	29.4	
3	PS	10.60	222.5	128.1	31.1	97.07
	PP	12.61	226.5	132.0	29.6	
4	PS	11.94	226.0	129.5	32.0	98.67
	PP	12.92	231.5	139.2	30.8	
5	PS	9.28	206.8	115.7	30.6	88.45
	PP	9.65	205.1	117.0	27.5	
6	PS	10.61	211.0	118.8	31.5	91.07
	PP	9.43	213.0	121.0	28.2	
7	PS	12.36	215.0	122.5	32.0	92.22
	PP	9.15	215.5	123.5	29.6	
8	PS	13.41	219.0	125.5	33.0	95.00
	PP	9.53	224.0	128.0	30.0	
9	PS	6.93	234.7	134.4	33.6	100.48
	PP	18.25	232.7	132.7	31.9	
10	PS	9.28	243.6	139.6	35.5	104.40
	PP	17.80	243.0	140.0	33.5	
11	PS	10.60	245.9	140.6	36.6	105.40
	PP	18.55	250.0	142.7	33.7	
12	PS	11.95	247.5	145.0	37.1	107.65
	PP	18.04	254.2	144.4	34.0	
13	PS	6.85	235.0	134.5	34.5	101.12
	PP	21.40	237.0	134.6	33.0	
14	PS	9.26	235.0	134.4	34.5	101.00
	PP	17.70	236.0	134.5	32.5	
15	PS	10.50	226.5	127.3	33.0	96.43
	PP	13.75	223.2	126.5	31.0	

[a] PS: Polystyrene (Dow Styron 686); PP: polypropylene (Enjay Chemical Resin E115).

[b] Refer to Fig. 5 for the locations of pressure measurements.

That is, the pressure gradients are also expected to be the same in both phases. This has been used already in the derivation of eqs. (2) and (3), and finally in eqs. (26) and (27).

It should be noted that White et al.[12] also predicted that the two pressure readings opposite each other in a slit die should be the same.

Figure 6 shows some representative plots of the axial distribution of wall normal stresses with total volumetric flow rate as a parameter. Note that in these plots the average values of the pressures of polystyrene and polypropylene melts were used. Two things are worth noting from the plots of Figure 6. First, the axial pressure distribution is a straight line over the distance where measurements were taken. Therefore, the slope of this straight line permits us to determine the effective wall shear stress of the

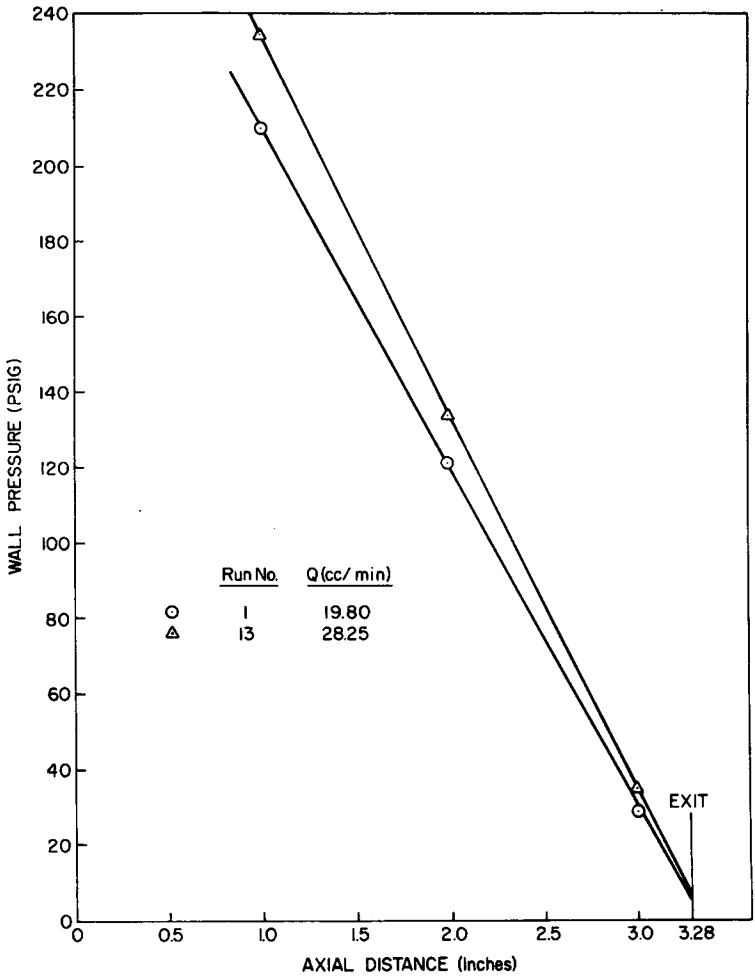

Fig. 6. Plots of the axial pressure distribution.

two-phase system investigated. Second, the extrapolation of the measurements taken nearest to the die exit gives rise to a nonzero exit pressure. This has been referred to as "exit pressure" by Han and his co-workers, who have made an extensive investigation of it during the past four years.[17-21] Because of the experimental evidence that wall pressures are the same in both phases (see Table I), the exit pressures also should be the same in both phases. More will be said later about the exit pressure.

Viscous and Elastic Effects

For comparison purposes, measurements of the wall normal stresses of individual components in single-phase flow are shown in Table II. It is clearly seen that, at comparable flow rates, wall pressures of polystyrene melts are much higher than those of polypropylene melts, and hence higher pressure gradients exist in polystyrene than in polypropylene.

TABLE II
Experimental Data of the Slit Flow of Pure Components

Material	Flow rate, cc/min	Wall pressure, psig			$-\partial p/\partial z$, psi/in.	τ_w, psi	γ_w, sec^{-1}	Exit pressure, psig	η, poise
		P_1	P_2	P_3					
Polystyrene	19.6	305.3	180.9	48.6	128.3	6.416	11.95	13.89	0.370×10^5
	37.0	385.4	225.7	61.5	161.9	8.095	22.58	16.78	0.247×10^5
	48.8	412.1	241.7	65.6	173.3	8.664	29.77	17.83	0.201×10^5
	55.7	426.9	250.9	67.9	179.5	8.974	33.95	18.66	0.183×10^5
	70.1	446.1	259.7	72.1	187.0	9.351	42.74	19.78	0.151×10^5
Polypropylene	26.6	176.0	105.8	29.3	73.4	3.67	16.2	9.69	0.156×10^5
	48.9	233.7	139.8	38.2	97.8	4.88	29.8	11.98	0.113×10^5
	57.6	254.2	150.3	41.3	106.4	5.32	35.1	12.28	0.104×10^5
	72.3	278.8	163.9	44.8	116.9	5.85	44.1	12.63	0.915×10^4
	89.0	298.9	176.1	48.0	125.5	6.27	54.3	13.63	0.796×10^4

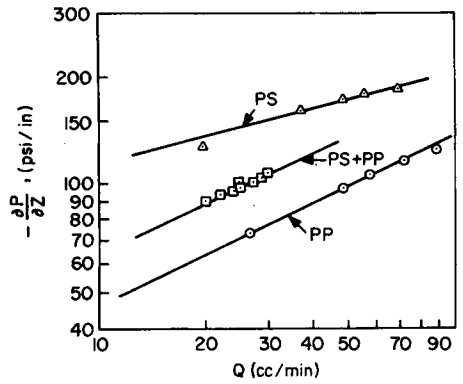

Fig. 7. Pressure gradients vs. volumetric flow rate for single- and two-phase systems.

Figure 7 shows plots of the pressure gradient versus volumetric flow rate for both single- and two-phase flow. It is seen that the pressure gradients of two-phase flow lie between those of two single-phase flows. This indicates that the presence of polypropylene, which is less viscous, brings a reduction in the pressure gradients of polystyrene, which is more viscous. Figure 8 shows cross plots of Figure 7, indicating that the pressure gradients of polystyrene melts are reduced by about 30%. This appears to be independent of the amount of polypropylene present in the two-phase system, say 30–70%. In Figure 8, the pressure gradient reduction factor (P.G.R.F.) is defined as the ratio of the pressure gradient of the two-phase system to that of the more viscous phase alone (in this case polystyrene), the flow rate being the same in each case:

$$\text{P.F.R.F.} = \left(\frac{-\partial p}{\partial z}\right)_{ps/pp} \Big/ \left(\frac{-\partial p}{\partial z}\right)_{ps}$$

for constant Q_T.

At this point, it is appropriate to point out the earlier studies by Charles and Lilleleht[3] and Gemmel and Epstein,[2] who reported that a drastic reduction of power requirement was observed in the transportation of heavy, viscous crude oil through a pipeline when a relatively small amount of water was injected into the pipeline. These authors contended that the observed reduction in power consumption was due to the reduction in pressure gradient caused by the preferential wetting of the pipe wall by the less viscous water. A similar situation has been known to the polymer processing industry which processes polymer blends containing low molecular weight materials as either lubricants or plasticizers. A prevailing theory for the observed reduction in pressure drops across the die is that low molecular weight materials tend to migrate toward the die wall, hence giving rise to much lower shear stresses at the wall.

Table III shows the observed effects of the component ratios on pressure gradients and exit pressures. It is seen that the pressure gradient (hence wall shear stress) is not sensitive to change in the polystyrene/polypropyl-

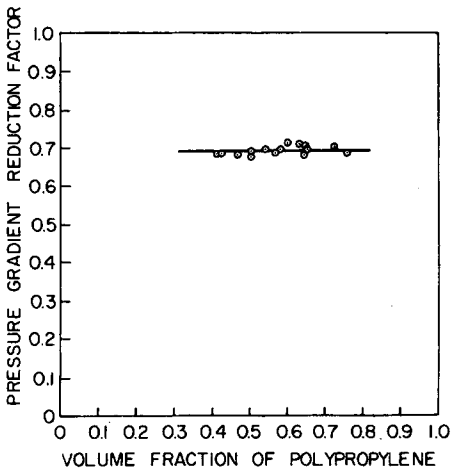

Fig. 8. Pressure gradient reduction factor vs. volume fraction of polypropylene.

ene ratio, and that the exit pressure increases as the amount of polystyrene is increased while keeping the total flow rate constant. This increase in exit pressure is as expected because Table II shows that at comparable flow rates, polystyrene gives higher exit pressures than polypropylene. According to Han and his co-workers,[17–21] the existence of the exit pressure is a manifestation of the elastic properties of the materials investigated. Hence, one can conclude from Table II that wall pressure measurements in stratified two-phase flow may be used to follow the changes in the elastic properties of mixtures due to changes in the component ratio, but not to follow the changes in the viscous properties.

TABLE III
Effect of the Component Ratio on Exit Pressure

Run no.	Q_t, cc/min	Q_{ps}/Q_t	$-\partial p/\partial z$, psi/in.	τ_w, psi	P_{exit}, psig
1	19.80	0.345	90.80	4.54	3.385
6	20.04	0.529	91.07	4.55	3.917
2	21.95	0.419	94.07	4.704	3.624
7	21.51	0.575	92.22	4.611	4.876
3	23.21	0.456	97.07	4.854	3.947
8	22.94	0.585	95.00	4.750	4.888

The present study shows further that the pressure gradient (a viscous property) is quite sensitive to changes in the total volumetric flow rate, as shown in Table IV. It is seen there that, for a fixed component ratio, both wall shear stress and exit pressure increase with total volumetric flow rate. Again, this is to be expected in view of the results shown in Table II for single-phase flow.

TABLE IV
Effect of the Total Flow Rate on Exit Pressure

Run no.	Q_t, cc/min	Q_{ps}/Q_t	$-\partial p/\partial z$, psi/in.	τ_w, psi	P_{exit}, psig
1	19.80	0.345	90.80	4.540	3.385
14	26.96	0.343	101.00	5.050	5.102
10	27.08	0.346	104.40	5.220	5.463

Comparison of Experimental with Theoretically Predicted Volumetric Flow Rate

The usefulness of the theoretical development given above may be evaluated by comparing the calculated volumetric flow rates with the experimentally observed ones. A comparison is given in Table V, in which the calculated flow rates are based on the power law model, that is, by use of eqs. (26) and (27).

TABLE V
Comparison of the Calculated with Experimentally Observed Volumetric Flow Rate

Run no.	Material	Experimentally observed flow rate, cc/min	Calculated flow rate, cc/min
1	PS	6.80	4.01
	PP	13.00	13.23
2	PS	9.20	6.32
	PP	12.75	11.74
3	PS	10.60	8.00
	PP	12.61	11.51
4	PS	11.94	9.15
	PP	12.92	11.21
5	PS	9.28	6.82
	PP	9.65	8.11
6	PS	10.61	8.32
	PP	9.43	7.87
7	PS	12.36	9.63
	PP	9.15	7.15
8	PS	13.41	10.74
	PP	9.53	7.50
9	PS	6.93	3.55
	PP	18.25	21.22
10	PS	9.28	6.05
	PP	17.80	19.20
11	PS	10.60	6.97
	PP	18.55	18.51
12	PS	11.95	8.71
	PP	18.04	17.78
13	PS	6.85	2.82
	PP	21.40	23.93
14	PS	9.26	5.52
	PP	17.70	17.51
15	PS	10.50	12.00
	PP	13.75	7.25

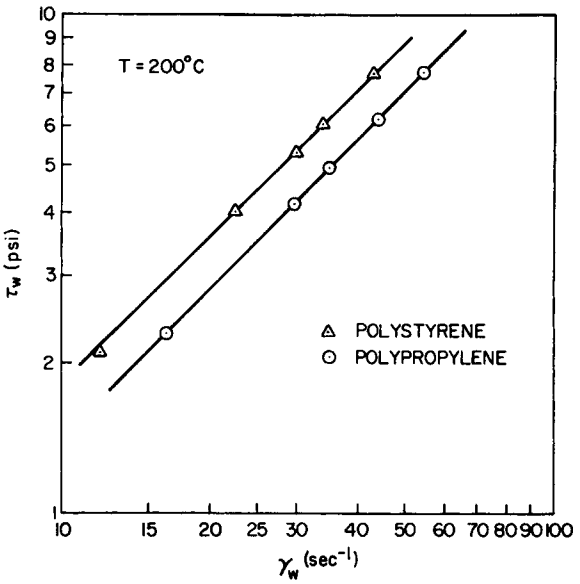

Fig. 9. Flow curves for polystyrene and polypropylene melts.

For computation, two material constants, K and n, in the power law model were determined for the individual components, polystyrene and polypropylene, respectively. This was done by preparing plots of the wall shear rate as shown in Figure 9, where τ_w and γ_w are defined by

$$\tau_w = \left(\frac{-\partial p}{\partial z}\right)\frac{B}{2} \tag{35}$$

$$\gamma_w = \frac{6Q}{WB^2} \tag{36}$$

respectively. Having established the fact that both polystyrene and polypropylene melts follow a power law, we obtained the two material constants K and n from

$$\tau_w = K\gamma^n \tag{37}$$

where γ is the true shear rate after the Rabinowitch-Mooney correction is properly made:

$$\gamma = \left(\frac{2n+1}{3n}\right)\gamma_w \tag{38}$$

in which $n = d \ln \tau_w / d \ln \gamma_w$. Table VI shows the numerical values of K and n for polystyrene and polypropylene melts, respectively, at 200°C.

It is seen from Table V that the calculated flow rates are consistently lower than the experimentally observed ones by about 10% in polypropylene and about 30% in polystyrene, on the average. However, they may be considered to be acceptable, considering the first three assumptions made

TABLE VI
Material Constants in Power Law Model

Material	Temp., °C	K, lb/in.^{2}-sec^{-n}	n (dimensionless)
Polystyrene	200	2.598	0.301
Polypropylene	200	0.902	0.451

in the theoretical development. The first is that the flow through a thin slit die (aspect ratio of 10 in the present study) is assumed to be one-dimensional, not two-dimensional. The second is that the phase interface is assumed to be a flat surface. The third is that the power law constants, K and n, of the individual components are assumed to hold in stratified two-phase flow. All of these assumptions have considerably simplified the mathematical manipulations for deriving the expressions for the volumetric flow rate. However, it is quite conceivable that any of these assumptions could have contributed to the difference between the calculated and measured flow rates. In particular, the latter two assumptions could play an important role in accurately determining the volumetric flow rate. At present, an experimental investigation is under way to help better understand the interfacial phenomenon in the two-phase flow of molten polymers.

Calculation of Velocity Distributions

The power law model was used further to calculate the velocity distributions in the stratified two-phase flow of polystyrene and polypropylene melts under the experimental conditions. Some representative results are shown in Figures 10 and 11.

Figure 10 shows the velocity distributions of two phases for different pressure gradients, keeping the polystyrene/polypropylene ratio the same. It is seen that, as expected, the larger the pressure gradients, the higher the local velocities are, while still maintaining the same shape of velocity profiles.

However, Figure 11 shows that a change in polystyrene/polypropylene ratio, keeping total volumetric flow rates constant, brings a change in shape of the velocity profiles. It should be noted, however, that the effective pressure gradients in the two cases are the same, although with different exit pressures (see Table III). This raises an interesting and important question. Is it valid to use two material constants, K and n, determined from wall shear stress measurements of the individual components, in order to predict the volumetric flow rate in stratified two-phase flow? After all, wall shear stresses determined by the use of wall pressure measurements are not sensitive to changes in the ratio of the two components.

It is expected, however, that a change of velocity profiles due to changes of polystyrene/polypropylene ratio may be attributable to changes in both viscous and elastic properties of the two materials flowing together, parallel to each other. At present, we are pursuing a study of how the

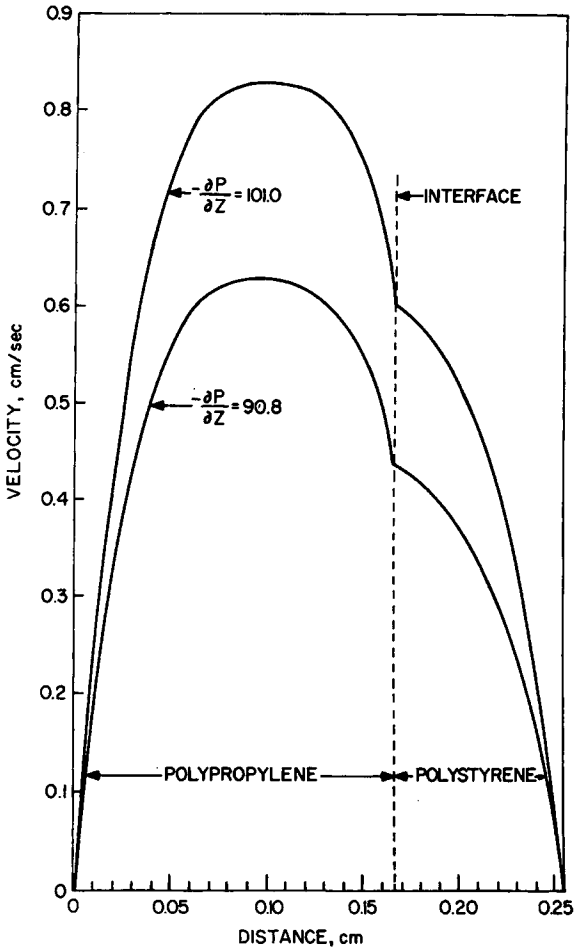

Fig. 10. Velocity distributions for different pressure gradients, keeping the polystyrene/polypropylene ratio constant.

interactions of two materials might be taken into account in order to correctly describe the flow behavior of two incompatible viscoelastic fluids.

Evidence of Incompatibility in the Polystyrene/Polypropylene System

In previous work, the authors[5,6] have shown that blends of polystyrene and polypropylene, when melted and extruded through a capillary die, exhibit complete incompatibility. For the sake of completeness, we present the pictures in Figure 12, which show the microstructure of extrudate samples obtained from a blend. Note that these pictures were taken as part of an earlier study which was concerned with the rheological properties of blend systems. In the blend, polystyrene forms the discrete phase (black portions of the picture), and polypropylene, the continuous phase (white portions). The fact that these two materials form two phases,

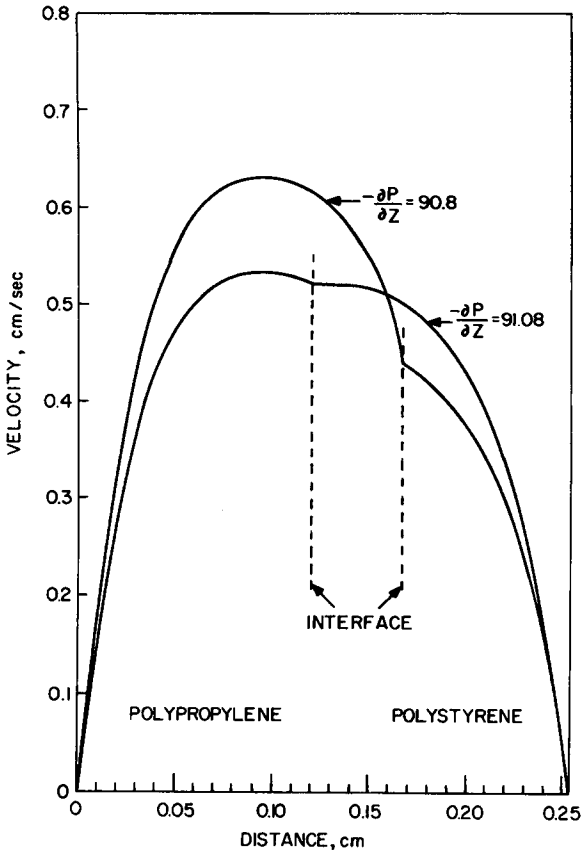

Fig. 11. Velocity distributions for different polystyrene/polypropylene ratios, keeping the total volumetric flow rate constant.

at least under the extrusion conditions, may be expected on the following two accounts: First, polystyrene belongs to the aromatic group (containing benzene rings), while polypropylene belongs to the aliphatic group (containing straight carbon chains); second, the residence time involved in the extrusion operation is considered to be too short to allow any sort of molecular diffusion. These macromolecules have extremely large values of viscosity (2000–4000 poises at 200°C) over the range of shear rates investigated.

Based on the pictures shown in Figure 12, one would then expect to have a completely stratified flow when polystyrene and polypropylene melts are fed separately to a die inlet and flow through the die. The authors have found that this was indeed the case when extrudate samples were collected and cross-sectioned. In fact, polystyrene and polypropylene initially forming a single piece of extrudate have split apart into two separate pieces when completely frozen. Figure 13 shows a picture of the cross section of separated extrudates of polystyrene and polypropylene.

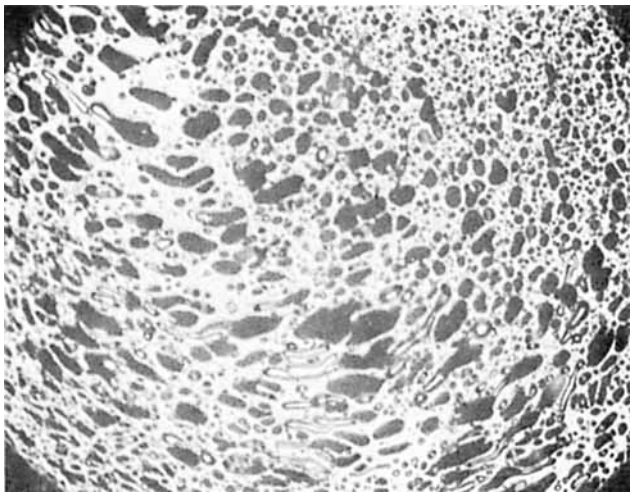

(a)

(b)

Fig. 12. Pictures (200×) showing the microstructure of an extrudate sample of 50 wt-% polystyrene/50 wt-% polypropylene blends, extruded in a circular tube of L/D = 20 (D = 0.125 in.) at 200°C: (a) middle portion of extrudate cross section; (b) middle portion of extrudate in the longitudinal direction.

It may be worth making a few observations on the picture in Figure 13. First, the interface is not really a well-defined flat surface; rather, it has a curvature. Second, the interface appears to have a mild corrugation. Interestingly enough, Yu and Sparrow[4] have observed a similar interface when they studied the stratified flow of two Newtonian fluids flowing through a rectangular duct. It should be noted, however, that the interface shown in Figure 13 might not be the one actually exiting in the die. While

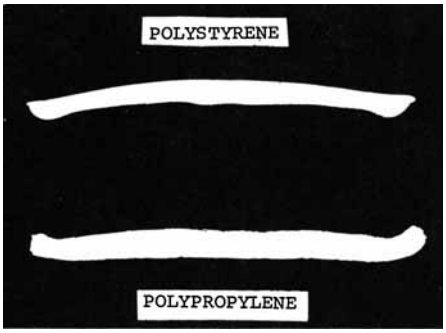

Fig. 13. Picture of extrudate cross section showing the phase interface in stratified flow of polystyrene and and polypropylene melts in a slit die at 200°C.

being cooled, the polypropylene, which is a crystalline polymer, would behave (i.e., shrink) differently from the polystyrene, which is an amorphous polymer. In other words, the rate of crystallization of polypropylene during cooling could alter the shape of the interface between two molten polymers, conceivably giving rise to corrugated, deformed interfaces in the frozen state.

At present, an experimental study is under way for making visual observations of the interface in fully developed, stratified two-phase flow of molten polymers, using a thin slit die made of a special quality of quartz.

CONCLUSIONS

An experimental and theoretical study has been carried out to investigate the stratified two-phase flow of molten polymers in a slit die. From the study, the following conclusions may be drawn:

1. Measurements of wall normal stresses in the two phases give the theoretically expected result, namely, the same wall pressures in both phases and consequently the same pressure gradients in both.

2. The effective wall pressure gradient of polystyrene, which is the more viscous, is reduced by about 30% in the presence of polypropylene over the range of component ratios investigated.

3. At a fixed volumetric flow rate of the combined stream, wall pressure measurements are insensitive to changes in the component ratio, but very sensitive to changes in the total volumetric flow rate. Wall pressures increase with flow rate.

4. Exit pressure is found to be sensitive to changes in both the total volumetric flow rate and component ratio.

5. Although the power law model cannot describe the elastic effects of molten polymers, which are viscoelastic in the present case, it enables us to calculate the volumetric flow and velocity profiles by solving the equations of motion. The volumetric flow rates, calculated theoretically by use of a power law model, are somewhat low compared to the experimen-

tally observed values. Reasons are given which might explain the discrepancy.

6. Further experimental evidence is presented which clearly shows that polystyrene and polypropylene form two incompatible phases in the molten state.

This work was supported in part by the National Science Foundation under Grant GK-23623, for which the authors are grateful.

Notation

B	thickness of the slot in a slit die
C	a position at which maximum velocity is attained
$K, \bar{K}$	material consistency of phases 1 and 2, respectively, in the power law fluid
$n,\bar{n}$	power law constant of phases 1 and 2, respectively
p	isotropic pressure
P'	pressure gradient defined by $-\partial p/\partial z$
Q_{ps}	volumetric flow rate of polystyrene
Q_{pp}	volumetric flow rate of polypropylene
Q_t	total volumetric flow rate
$Q,\bar{Q}$	volumetric flow rate of phases 1 and 2, respectively
$S_{yy},\bar{S}_{yy}$	total normal stress in the y-direction of phases 1 and 2, respectively
$V, \bar{V}$	velocity profiles of phases 1 and 2, respectively
W	width of the slot in a lit die
τ_w	wall shear stress
γ_w	apparent shear rate
γ	true shear rate
ρ	fluid density
α	a location of phase interface

References

1. T. W. F. Russel and M. E. Charles, *Can. J. Chem. Eng.*, **37**, 18 (1959).
2. A. R. Gemmell and N. Epstein, *Can. J. Chem. Eng.*, **40**, 215 (1962).
3. M. E. Charles and L. U. Lilleleht, *Can. J. Chem. Eng.*, **43**, 110 (1965).
4. H. S. Yu and E. M. Sparrow, *ASME Trans. C*, **91**, 51 (1969).
5. C. D. Han and T. C. Yu, *J. Appl. Polym. Sci.*, **15**, 1163 (1971)
6. C. D. Han and T. C. Yu, *Polym. Eng. Sci.*, **12**, 81 (1972).
7. W. E. Sisson and F. F. Morehead, *Text. Res. J.*, **23**, 152 (1953); *ibid.*, **30**, 153 (1960).
8. E. M. Hicks, J. F. Ryan, R. B. Taylor, and R. L. Tichenor, *Text. Res. J.*, **30**, 675 (1960).
9. E. M. Hicks, E. A. Tippets, J. V. Hewett, and R. H. Brand, in *Man-Made Fibers*, Vol. 1, H. Mark, S. M. Atlas, and E. Cernia, Eds., Interscience, New York, 1967.
10. R. A. Buckley and R. J. Phillips, *Chem. Eng. Progr.*, **66** (No. 10), 41 (1969).
11. J. H. Southern and R. L. Ballman, paper presented at the 163rd ACS Annual Meeting, Boston, Mass., April 1972.
12. J. L. White, R. C. Ufford, K. R. Dharod, and R. L. Price, *J. Appl. Polym. Sci.*, **16**, 1313(1972).

13. J. C. Slattery. *A.I.Ch.E. J.*, **10**, 817 (1964).
14. W. Noll, *Arch. Rat'l Mech. Anal.*, **2**, 197 (1958).
15. B. D. Coleman and W. Noll, *Arch. Rat'l Mech. Anal.*, **6**, 355 (1960).
16. C. D. Han and R. R. Lamonte, *Trans. Soc. Rheol.*, **16**, 447 (1972).
17. C. D. Han, M. Charles, and W. Philippoff, *Trans. Soc. Rheol.*, **13**, 455 (1969).
18. C. D. Han, M. Charles, and W. Philippoff, *Trans. Soc. Rheol.*, **14**, 393 (1970).
19. C. D. Han, T. C. Yu, and K. U. Kim, *J. Appl. Polym. Sci.*, **15**, 1149 (1971).
20. C. D. Han and K. U. Kim, *Polym. Eng. Sci.*, **11**, 395 (1971).
21. C. D. Han and R. R. Lamonte, *Polym. Eng. Sci.*, **11**, 385 (1971).

Received August 4, 1972